Relevance Rank Platform (RRP) for Functional Filtering of High Content Protein–Protein Interaction Data*[S]

Yuba Raj Pokharel‡§‖‡‡, Jani Saarela‡‡‡, Agnieszka Szwajda‡‡‡, Christian Rupp§, Anne Rokka§, Shibendra Kumar Lal Karna‖, Kaisa Teittinen, Garry Corthals§, Olli Kallioniemi‡, Krister Wennerberg‡, Tero Aittokallio‡, and Jukka Westermarck‡§¶§§**

High content protein interaction screens have revolutionized our understanding of protein complex assembly. However, one of the major challenges in translation of high content protein interaction data is identification of those interactions that are functionally relevant for a particular biological question. To address this challenge, we developed a relevance ranking platform (RRP), which consist of modular functional and bioinformatic filters to provide relevance rank among the interactome proteins. We demonstrate the versatility of RRP to enable a systematic prioritization of the most relevant interaction partners from high content data, highlighted by the analysis of cancer relevant protein interactions for oncoproteins Pin1 and PME-1. We validated the importance of selected interactions by demonstration of PTOV1 and CSKN2B as novel regulators of Pin1 target c-Jun phosphorylation and reveal previously unknown interacting proteins that may mediate PME-1 effects via PP2A-inhibition. The RRP framework is modular and can be modified to answer versatile research problems depending on the nature of the biological question under study. Based on comparison of RRP to other existing filtering tools, the presented data indicate that RRP offers added value especially for the analysis of interacting proteins for which there is no sufficient prior knowledge available. Finally, we encourage the use of RRP in combination with either SAINT or CRAPome computational tools for selecting the candidate interactors that fulfill the both important requirements, functional relevance, and high confidence interaction detection. ***Molecular & Cellular Proteomics 14: 10.1074/mcp.M115.050773, 3274–3283, 2015.***

Development of high content methods for protein interaction identification have dramatically increased our understanding of organization of cellular protein complexes (1). In addition, development of web-based protein interaction network analysis platforms such as Protein Interaction Network analysis has greatly helped construction, filtering, and analysis of protein interactomes (2). Regardless of these advances, one of the major challenges in protein–protein interaction screens is to dissociate from large number of interactions those that are functionally relevant for a particular biological question. Moreover, even though currently used quantitative methods emphasize the importance of repeatability in weighting the likelihood of an identified interaction to be true (3, 4), we cannot exclude even one-time identification of a few peptides of a previously unknown protein, as they may lead to the discovery of an entirely new biological concept, provided the identified interaction and its functional relevance is properly verified by subsequent experimentation (1, 5–7). Finally, when considering the reliability of the identified putative interaction, the functional classification of candidate interactors to "relevant" *versus* "nonrelevant" may not be advisable without further supporting data. Protein interactions of signaling proteins with cytoskeletal proteins are the classical examples of such interactions that might be omitted using such classification, notwithstanding the vast literature of relevance of these interactions for regulation of cellular signaling (1).

Taking into account these serious concerns, we rationalized that it would be useful to develop a method that could advise, regardless of either the reliability of the MS-based identification or known biological function of the putative interactor, what are the proteins from the high content screens that most likely contribute to the function of the bait protein. This could direct the choice of proteins for subsequent validation and functional experiments, optimally without the need to first verify the protein–protein interaction between the bait and candidate proteins. We envision that this would be especially

From the ‡Institute for Molecular Medicine Finland FIMM, University of Helsinki, PO Box 20, FIN-00014 Helsinki, Finland; §Centre for Biotechnology, ¶Department of Pathology,University of Turku and Åbo Akademi, Turku, Finland, PO Box 123, FIN-20521 Turku, Finland.; ‖Faculty of Life Science and Biotechnology, South Asian University, New Delhi 110021, India; **Institute of Biosciences and Medical Technology (BioMediTech), University of Tampere and Tampere University Hospital, FIN-33014, Tampere, Finland

Received April 16, 2015, and in revised form, September 30, 2015
Published October 23, 2015, MCP Papers in Press, DOI 10.1074/mcp.M115.050773

Author contributions: Y.R.P., J.S., O.K., K.W., T.A., and J.W. designed the research; Y.R.P., J.S., A.S., C.R., A.R., S.K., and K.T. performed the research; Y.R.P., J.S., A.S., A.R., G.C., K.W., T.A., and J.W. analyzed data; A.S., T.A., and J.W. wrote the paper; and G.C. supervised the MS analysis.

useful for analysis of proteins for which existing prediction programs such as FunCoup (8), which infer genome-wide functional couplings, would not be useful due to the limited amount of supporting literature or functional data.

In order to develop such a filtering tool for high content protein–protein interaction data, we considered that an affordable and rapid combination of approaches would involve functional siRNA screens combined with bioinformatic filters. As a relevant read-out for the proof-of-principle test, we chose oncogenic function of established oncoproteins Pin1 (9, 10) and PME-1 (11). The resulting platform, designed as relevance rank platform (RRP)[1], consists of several subsequent filtering steps, each of which produces a ranking, and whose combination then determines the final RRP rank between the interactome proteins. More specifically, RRP ranks each interacting protein in the order of its increased likelihood of contributing to the oncogenic activity of the bait, without taking into account any information regarding reliability of MS detection or other interaction quality measurements. This rank is collectively called a "similarity rank." Detailed descriptions of the specific rankings are shown in Fig. 1 and in Supplemental Table 1.

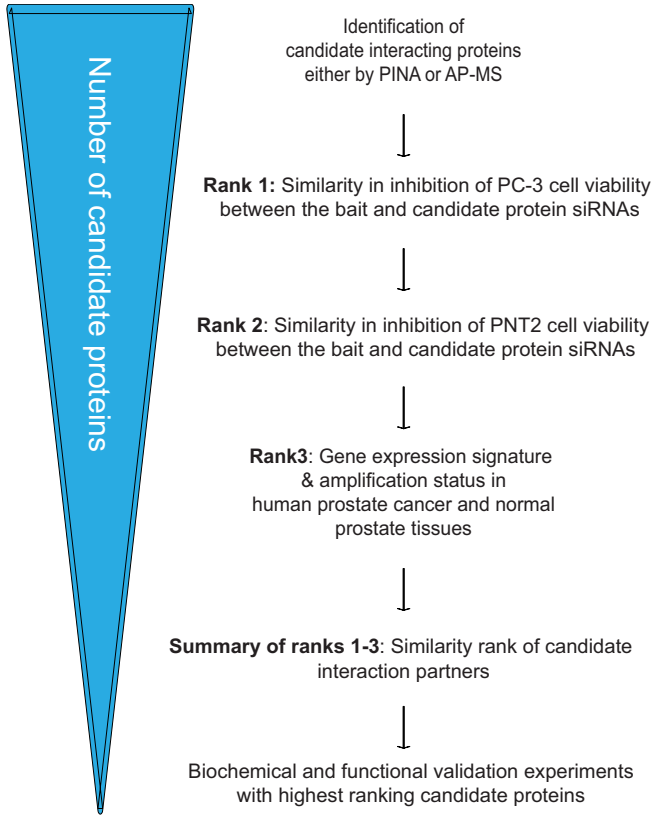

FIG. 1. **Schematic presentation of *r*elevance *r*ank *p*latform (RRP) principle.**

EXPERIMENTAL PROCEDURES

Cell Culture—Prostate cancer cell line (PC3) was cultured in RPMI containing 10% FBS and 1% penicillin–streptomycin antibiotic in 10 cm cell culture dishes. The cells were grown up to 90% confluence in incubator at 37 °C and 5% CO_2. For colony formation assay, PC3 cells were transfected with siRNA for 48 h and plated into three 6-cm cell culture dishes (1,000 per dish). Cells were incubated for 15 days in medium containing 10% FBS. Plates were washed with PBS, fixed in 3.7% formaldehyde, and stained with crystal violet.

High-throughput RNAi Screening for Cell Proliferation Effects—Custom human siRNA library was acquired from Qiagen on 384-well plates with three non-overlapping siRNAs targeting each gene. Library and control siRNAs were transferred to black clear bottom tissue-culture-treated 96-well plates (Costar #3904) using acoustic droplet ejection method with Echo 550 liquid handler (Labcyte, Sunnyvale, CA). The assay plates were used right away or used later, in which case they were kept sealed in −20 °C until used. Prior to transfection, 20 μl of Optimem medium (Gibco, Grand Island, NY) containing 125 nl of Lipofectamine 2000 (Invitrogen) per well was added using Multidrop Combi nL (Thermo Scientific, Waltham, MA), and plates were mixed for 15–90 min. After mixing, 500 cells per well were added in 80 μl of culture medium using Multidrop Combi (Thermo Scientific). Final concentration of siRNA in assay plates was 12 nM. After transfection, cells were incubated at 37 °C for 7 days in the presence of 5% CO_2 in cell incubator (HERACell 240, Thermo Scientific). Cell proliferation was measured by adding 100 μl per well of CellTiter-Glo (Promega, Madison, WI) followed by shaking for 5 min at 600 rpm (Titramax 1000, Heidolph) and centrifugation for 5 min at 1,000 rpm (SL40R, Thermo Scientific), and luminescence was detected using Pherastar FS plate reader (BMG Labtech, Baden-Württemberg, Germany). The controls used in the screens were from Qiagen or Eurofins MWG. As negative control AllStars negative and as positive control AllStars Death control were used with four replicates per plate of each. As internal controls, siRNAs targeting Pin1, PME1, and CIP2A were used with four replicates per plate of each control. For each plate, the following calculations were performed to obtain relative inhibition values for all wells (% inhibition = $100*((average_{neg}-average_{sample})/(average_{negative}-average_{positive}))$). Z' was calculated for all plates with the following formula: $Z' = 1-3*((stdevp_{positive}-stdevp_{negative})/abs\ (average_{positive}-average_{negative}))$. Z' values for the screens performed are included in Supplemental Table 2.

RRP Similarity Rankings—To identify the set of genes most functionally related to PIN1 and PME-1, we calculated a similarity ranking, which combines complementary information from three functional assays into a single ranking of genes. In the first ranking, the siRNAs were ranked according to their difference in percentage inhibition levels from the average PIN1, or PME-1 siRNA % inhibition in PC-3 cells, so that the siRNA with the lowest absolute difference obtained the top rank equal to 1. In the second ranking, the siRNAs were ranked similarly as in the first ranking but using the average percent-

[1] The abbreviations used are: RRP, relevance ranking platform; Pin1, peptidyl-prolyl cis-trans isomerase NIMA-interacting1; PME-1 (PPME1), protein phosphatase methylesterase1; AP-MS, affinity purified-mass spectrometry; CSNK2B, casein kinase 2, beta polypeptide; PTOV1, prostate tumor overexpressed1; MYC, avian myelocytomatosis viral oncogene homolog; CDC27, cell division cycle 27; NONO, non-POU-domain-containing, octamer-binding; CDK1, cyclin dependent kinase1; PP2A, protein phosphatase 2 A; PR65, protein phosphatase 2, regulatory subunit A (PR 65), alpha; PP2AC, protein phosphatase 2A, catalytic subunit; PKM2, pyruvate kinase muscle; MS, mass spectrometry; MAPK3 (ERK1), mitogen activated protein kinase3 (extracellular signal-regulated kinase1); AKT1, v-Akt murine thymoma viral oncogene homolog1; CRAPome, Contaminant Repository for Affinity Purification; HSPA8, heat shock 70 kDa protein 8; FDPS, farnesyl diphosphate synthase; HRNR, hornerin; ERp72, endoplasmic resident protein 72; CIP2A: cancerous inhibitor of PP2A.

age inhibition measured in the PNT2 cells instead of that in the PC-3 cells and again giving the top rank to the siRNA with the smallest absolute difference. The third ranking was based on expression similarity with PIN1 and PME-1 using expression profiles of clinical samples both in prostate adenocarcinoma and healthy tissue from the MediSapiens database (http://www.medisapiens.com/) (12). Finally, we took a statistical approach, redundant siRNA activity analysis (13), which takes into account potential off-target activities by considering the enrichment of ranks of the siRNAs targeting the same gene, when moving from individual siRNAs to the final gene-level similarity ranks.

Reagents and Antibodies—RPMI (11875–119), FBS (10082147), and immunoprecipitation kit-Dynabeads-Protein G (10007D) were purchased from Life Technologies. Penicillin–streptomycin 100x (A001A) solution was purchased from Himedia. The antibodies against PIN1 (H-123:SC-15340), c-Jun, MYC, FTSJ1 (B-2:SC-390355), DDX24 (C-12:SC-104863), FNBP3 (D-20:SC-68080), PME-1 (B-12: SC-25278), Lamin A/C, (H-110 SC-20681; H-110), rabbit anti goat IgG-HRP (SC-2922), and normal rabbit IgG (SC-2027) were purchased from Santa Cruz Biotechnology. PP2Ac antibody was from Cell Signaling (#2038). The antibodies against anti-mouse IgG-HRP(A9044), anti-rabbit IgG(A0545) were purchased from Sigma Life Science.

Immunoprecipitation and Strep-Tag Pull-Down Experiments—The cells were washed with cold PBS two times and collected in PBS using a scraper. The cells were centrifuged at 6000 rpm for 5 min. The cells were lysed in lysis buffer (50 mM Tris (pH 7.5), 5 mM EDTA, 150 mM NaCl, 1 mM dithiothreitol, 0.01% Nonidet P-40, 0.2 mM phenylmethylsulfonyl fluoride, and 1X protease inhibitor mixture). The cells were sonicated for 10 s. The cells were again centrifuged for 15,000 rpm for 20 min at 4°C. The supernatant was collected in an Eppendorf tube. 50 μl of lysate was collected for input. Remaining cell lysate was divided into two equal parts in two Eppendorf tubes and made 1 ml using lysis buffer and labeled as Pin1 IP and normal rabbit IgG. The lysates were incubated with 2 μg of Pin1 and normal rabbit IgG in respective tubes at 4°C with gentle rolling for 12–24 h. On the next day, homogenous solution of magnetic beads were taken in two Eppendorf tubes and placed in a magnet. The supernatant was thrown. The lysates containing antibody complex were incubated with the beads for 1 h at 4°C with gentle rolling. Again, the tubes were placed in the magnet and the supernatant was thrown. The beads were washed with 200 μl of washing buffer for five times by gentle pipetting with ice incubation for 30 s in each wash. The tubes were placed in a magnet, and the supernatant was thrown. This was repeated for five times. The samples along with input were heated with 2XSDS sample buffer for 5 min at 100°C. The samples were again placed in the magnet, and the supernatant was collected in new tubes. The input (2% of lysate volume), PIN1 IP and normal rabbit IgG, was loaded on 10% SDS-PAGE and subjected to electrophoresis.

For PME-1 interaction validation pull-downs, two 10 cm dishes of PC-3 cells were transfected with 15 μg plasmid DNA (pcDNAStrepIII, pcDNA_PME-1StrepIII, and pcDNA_PME-1R369DStrepIII) and 30 μl Lipofectamin 2000 (Life Technologies, Foster City, CA). 48 h, transfection cells were harvested, resuspended in 2 $\times$ 1 ml membrane lysis buffer (11), and mechanically disrupted. Lysates were cleared by centrifugation, and strep purification from subsequent supernatants was performed using 0.2 ml Strep-Tactin Superflow columns (IBA) following the manufacturer's instructions. Primers for site-directed mutagenesis (R369D mutant): forward: 5′-ACTTTCCTGATCGACCACAGGTTTGCAGAA-3′ reverse: 5′-TTCTGCAAACCTGTGGTCGATCAGGAAAGT-3′. The QuikChange site-directed mutagenesis kit (Agilent) was used to introduce the point mutation.

Proximity Ligation Assay—The proximity ligation assay was performed according to manufacturer protocol (Olink Bioscience, Uppsala, Sweden). Briefly, cells plated on coverslips were grown to 70% confluence, fixed for 10 min in 4% PFA followed by 10 min permeabilization in TBS, 0.1% Triton. Subsequently, the sample was blocked with blocking solution and incubated in a preheated humidity chamber for 30 min at 37 °C, followed by incubating primary antibodies (in blocking solution) overnight at 4 °C. Subsequently, cells were washed with Buffer A, and a PLA probe was incubated in a preheated humidity chamber for 1 h at 37 °C followed by ligase reaction in a preheated humidity chamber for 1 h at 37 °C. Next, amplification-polymerase solution for PLA, followed by incubating cells in a preheated humidity chamber for 100 min at 37 °C.

Western Blot Analysis—Samples for Western blotting were collected in SDS-PAGE sample buffer (1* SDS sample buffer: 62.5 MM Tris-HCL (pH 6.8 at 25°C), 2% w/v SDS, 10% glycerol, 50 mM DTT, 0.01% w/v bromphenol blue), boiled for 5 min, and centrifuged for 10 min at 10,000*g to remove insoluble material. After, SDS-PAGE proteins were transferred on to a nitrocellulose membrane. The antibody concentration and reaction with primary and secondary antibody was done according to the manufacturer's instructions. The proteins were visualized by enhanced chemiluminescence with either the Super-Signal West Femto Maximum Sensitivity Substrate (Pierce Biotechnology, Inc.) or the Proteome Grasp ECL Kit (Pierce Biotechnology, Inc.)

AP-MS Analysis of PME-1 Interactome—To identify PME-1 associated proteins, we established stable HT-1080 cell clones expressing either StrepPME-1 fusion protein or Strep-tag alone. The protein complex purification and MS identification were done as described earlier (14, 15). Briefly, cells were lysed in membrane lysis buffer and homogenized with ten strokes of a tight-fitted pestle in a dounce homogenizer. Lysate was centrifuged for 1 h at 100.000 g at +4 C. 1 ml Strep-Tactin Superflow columns were used for complex purification. After washes, the proteins were eluted with the provided elution buffer and fractions were collected. Proteins separated on 10% Bis-Tris gel using MOPS running buffer (BioRad, Hercules, CA) were silver stained, and the protein bands that showed visually enrichment in StrepPME-1 samples as compared with Strep-tag samples were isolated from both lanes for MS analysis. Following trypsin digestion, the LC-MS/MS analysis was performed on a nanoflow HPLC system (CapLC, Waters, San Diego, CA) coupled to a QSTAR Pulsar mass spectrometer (Applied Biosystems/MDS Sciex, Canada) equipped with a nanoelectrospray ionization source (Proxeon, Odense, Denmark). Peptides were first loaded on a trapping column (0.3 $\times$ 5 mm PepMap C18, LC Packings) and subsequently separated inline on a 15 cm C18 column (75 μm $\times$ 15 cm, Magic 5 μm 100 Å C18, Michrom BioResources, Inc., Sacramento, CA). The mobile phase consisted of water/acetonitrile (98:2 (v/v)) with 0.2% formic acid (solvent A) or acetonitrile/water (95:5 (v/v)) with 0.2% formic acid (solvent B). A linear 25-min gradient (from 2% to 35% B) was used to elute peptides. The flow rate was 200 nl/min.

MS data were acquired automatically using Analyst QS 1.1 software (Applied Biosystems/MDS SCIEX, Ontario, Canada). An information-dependent acquisition method consisted of a 1 s TOF MS survey scan of a mass range 350–1600 amu and 2 s product ion scan of a mass range 50–2000 amu. The two most intensive peaks over 20 counts with charge state 2–3 were selected for fragmentation.

Data were searched against the SwissProt database (version 57.6) using in-house Mascot (version 2.2.06). The Mascot search settings included a taxonomy filter "human," trypsin as an enzyme, precursor-ion mass tolerance of 0.3 Da, fragment-ion mass tolerance of 0.3 Da, one missed trypsin cleavage, and variable modifications of carbamidomethylation of cysteine and methionine oxidation. A significance threshold of $p < 005$ was used. Mascot search results were imported to Scaffold (v. 3.0, Proteome Software) for data evaluation.

SAINT and FunCoup Analyses—Mascot search results were uploaded to the Prohits platform (16) for further analysis using default settings. The files were subsequently merged by applying the sum of

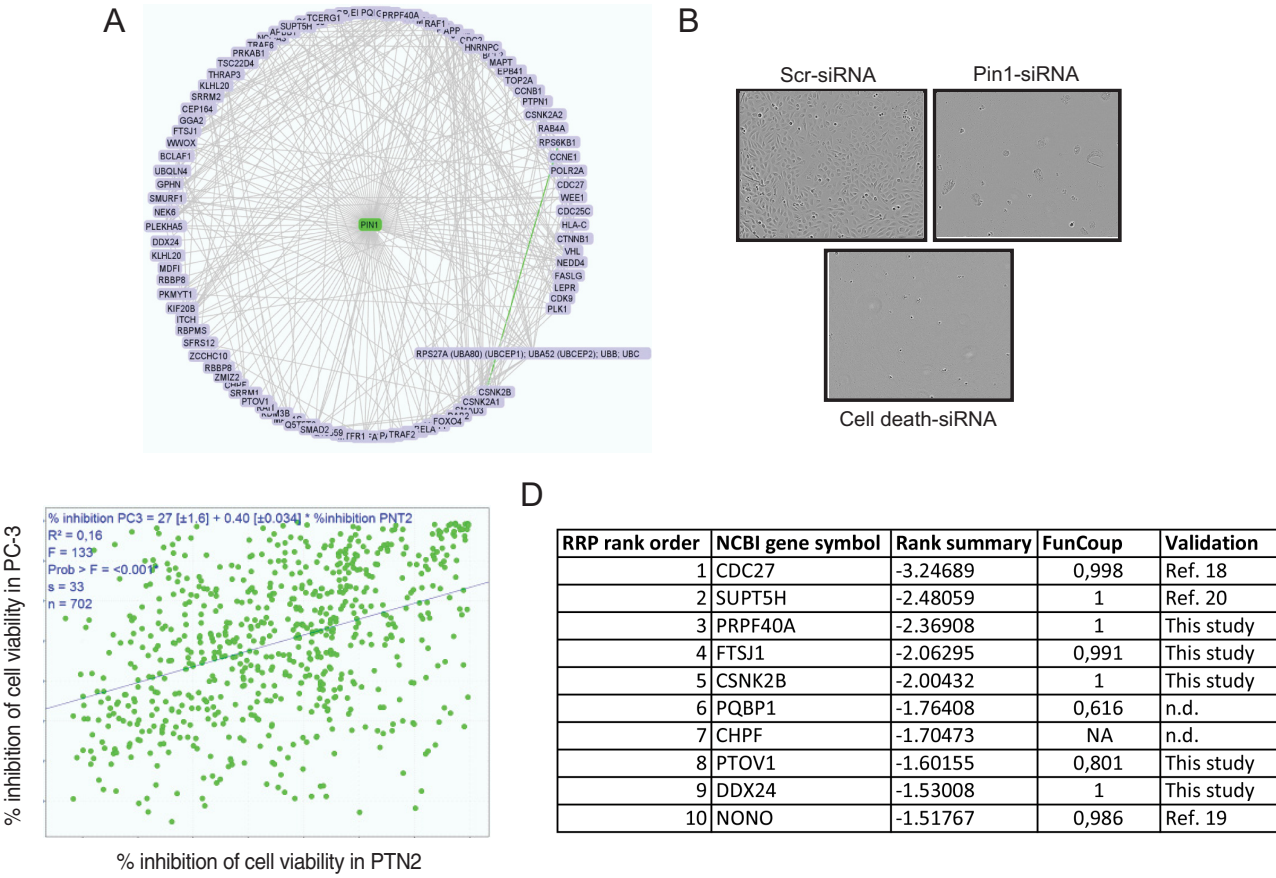

RRP rank order	NCBI gene symbol	Rank summary	FunCoup	Validation
1	CDC27	-3.24689	0,998	Ref. 18
2	SUPT5H	-2.48059	1	Ref. 20
3	PRPF40A	-2.36908	1	This study
4	FTSJ1	-2.06295	0,991	This study
5	CSNK2B	-2.00432	1	This study
6	PQBP1	-1.76408	0,616	n.d.
7	CHPF	-1.70473	NA	n.d.
8	PTOV1	-1.60155	0,801	This study
9	DDX24	-1.53008	1	This study
10	NONO	-1.51767	0,986	Ref. 19

FIG. 2. **RRP analysis of Pin1 interactome.** (*A*) Graphical presentation of analyzed Pin1 interactome based on: Protein Interaction Network analysis (2). (*B*) Phase contrast microscopy images of PC-3 cells transfected with indicated siRNAs on 384-well plate. (*C*) Graphical presentation of correlation of cell viability effects of individual siRNAs in PC-3 and PNT2 cells. (*D*) RRP ranking of top ten proteins with most similar function to Pin1. FunCoup similarity index (min. 0, max. 1) indicates for very high similarity in function with Pin1 for most RRP top ranked proteins. NA, not applicable due to lack of sufficient database information. Validation indicates either physical or functional validation for indicated interaction. N.d., not determined.

spectral counts for all samples from the same biological replicate. The data for the two biological PME1 bait replicates and controls were then analyzed using the SAINT express algorithm (3) to assess the interactions' reliability.

Functional coupling scores were extracted for the interaction partners of PME1 and Pin1 from the FunCoup database (8) using evidence from all available species and from human only, respectively.

RESULTS

RRP Analysis of Pin1 Interactome—In prostate cancer, Pin1 has a prognostic role (9), and it enhances tumor growth in immunodeficient mice (10). We verified the oncogenic role of Pin1 in supporting colony growth and MYC expression in widely utilized prostate cancer PC-3 cells (Supplemental Fig. 1). Therefore, this cell line was chosen as a model in which to assess the usefulness of RRP in selecting among the Pin1 interactome those proteins that are relevant for its function.

Based on integrated protein interactome database, Protein Interaction Network analysis (2), Pin1 had 88 interacting proteins (Fig. 2*A* and Supplemental Table 3) at the time this work was initiated. As the first rank, an siRNA library consisting of three individual siRNAs (Supplemental Table 4) against Pin1 (bait) and each of its interacting proteins was used to screen for cell viability effects in high-throughput 384-well plate format in PC-3 cells. As shown in Fig. 2*B*, Pin1 depletion caused marked cell death also in these assay conditions, visualized by phase contrast microscopy image of a 384-well plate. Cell viability assay values for knockdown of Pin1 interacting proteins and their corresponding ranking 1 values are shown in Supplemental Table 4. For the rank 2, we examined the context dependence of Pin1 interactome by studying the cell viability effects of Pin1 and its interactome in immortalized prostate epithelium PNT2 cell line (Fig. 2*C*). The effects of inhibition of Pin1 interacting proteins in PNT2 cells and the corresponding ranking 2 values are shown in Supplemental Table 4. As an additional indicator of functional similarity (rank 3), we next calculated the sum of expression profile correlations, here based on the expression data from MediSapiens database (12) (www.medisapiens.com), between bait (Pin1) and interacting proteins in malignant and normal prostate tissues. Relevance of this ranking is sup-

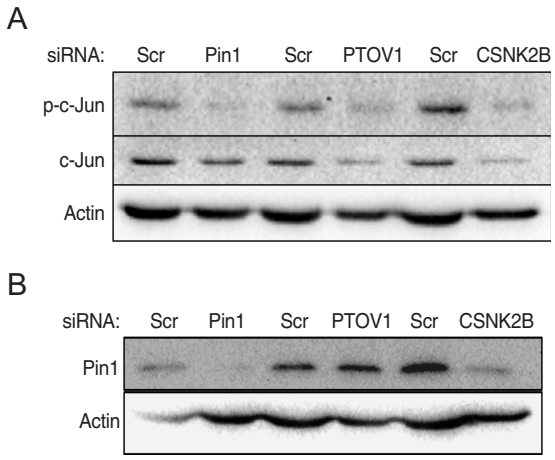

FIG. 3. **Validation of CSKN2B and PTOV1 as functional Pin1 interacting proteins.** (*A*) Western blot analysis of phosphorylated c-Jun expression in PC-3 cells depleted of either Pin1, PTOV, or CSKN2B. (B) Western blot analysis of Pin1 expression in PC-3 cells transfected either with Pin1, PTOV, or CSKN2B siRNAs.

ported by the well-established findings that genes that share biological functions show also coexpression *in vivo* (17). Finally, we took a statistical approach, redundant siRNA activity (13), which ensures that the genes with multiple moderately active siRNAs were weighted more than the ones with only one effective siRNA, to move from individual siRNAs to the final gene-level similarity ranks. The final RRP similarity rank order between Pin1 interacting proteins is shown in Fig. 2*D* and Supplemental Table 5.

Validation of CSKN2B and PTOV1 as Functional Pin1 Interacting Proteins—All proteins selected for Pin1 RRP analysis were selected based on their previous identification as Pin1 interacting proteins (2). Importantly, the top RRP ranked protein with highest predicted similarity to Pin1 function was CDC27 (Fig. 2*D*), which is an established Pin1 target involved in mitosis regulation (18). Also, interaction between SUPT5H and NONO with Pin1 has been validated previously by pull-down experiments (19, 20). In addition, we validate here protein interaction between Pin1 and PRPF40A, FTSJ1, CSNK2B, PTOV1, and DDX24 in PC3 cells (Supplemental Fig. 2 and Fig. 2*D*).

To further substantiate the capacity of RRP to rank interacting proteins based on their functional relevance to bait, we assessed the effects of depletion of Pin1 and two of the RRP top ten ranked proteins with no previously demonstrated association with Pin1 function, CSKN2B and PTOV1, for expression of AP-1 transcription factor c-Jun phosphorylated on transactivating serines 62 and 72 (21), as Pin1 promotes transcriptional activity of c-Jun (22). Notably, RNAi-mediated depletion of Pin1, CSKN2B, or PTOV1 each substantially inhibited expression of phosphorylated c-Jun (Fig. 3*A*). Interestingly, whereas PTOV1 depletion did not affect Pin1 proteins levels, CSKN2B RNAi resulted in very potent inhibition of Pin1 expression (Fig. 3*B*). To further challenge the hypothesis, we analyzed the Pin1 interactome by FunCoup analysis (8). Importantly, the relatively high average FunCoup value of 0,91 for the top ten RRP ranked Pin1 interacting proteins, except for CHPF for which there is not sufficient functional information available, validates that RRP is able to rank the interacting proteins with highest likelihood of being relevant to the bait function (Fig. 2*D* and Supplemental Table 6). In fact, analysis of the entire Pin1 interactome with FunCoup showed a significant correlation between the capacity of these two methods to rank functional similarity of Pin1 and its interactome in those cases where the interaction partner was available in the FunCoup database (Spearman correlation = -0.32, $p = .018$, Supplemental Table 6).

Taken together, functional relevance in Pin1 biology has been validated for 4/10 of the highest ranked Pin1 interacting proteins (CDC27, NONO, CSKN2B, and PTOV1), and protein interaction have been validated for 8/10 of the highest RRP ranked Pin1 interacting proteins. Together with comparison to FunCoup analysis (Fig. 2*D* and Supplemental Table 6), this provides a proof-of-concept demonstration of RRP's potential to supervise the selection of bait-relevant interacting proteins for follow-up experiments from high-content protein interactome data.

AP-MS Identification of PME-1 Interactome—Pin1 was selected as an example case to probe performance of RRP analysis because it has a well-established interactome that allows assessment of both the reliability of the interaction data, as well as the use of FunCoup and functional validation experiments. To further test the robustness of RRP to guide the selection of bait-relevant interacting proteins, we started from high-content protein interactome that has not been subjected to prefiltering for the reliability of protein interaction identification, using a bait protein for which there is limited published information available. To this end, we set up to purify a *de novo* protein complex by one-step Strep-tag method (15). PME-1 (PPME1) is a methylesterase that promotes ERK pathway activity in human glioblastoma by inhibition of protein phosphatase 2A (PP2A) (11). For single-step affinity purification coupled with mass spectrometry (AP-MS) identification of PME-1 interactome, we established a cell line stably expressing either Strep-tag alone (Strep) or Strep-PME-1 fusion protein. Both PP2A scaffold protein PR65 and the catalytic subunit PP2Ac were found to copurify with Strep-PME-1 (Fig. 4*A*), whereas neither of these were detected in the eluates of control Strep cells (Supplemental Fig. 3*A*). Moreover, unrelated protein PKM2 did not copurify with PME-1, indicating that the chosen one-step purification conditions show some selectivity for specific interactions (Fig. 4*A*). In a large-scale AP-MS experiment, silver-stained bands that visually showed enrichment in Strep-PME-1 samples as compared with an adjacent Strep control lane in any of the three experiments (Fig. 4*B* and Supplemental Figs. 3*B*, 3*C*, and 3*D*) were subjected to MS identification. As some low

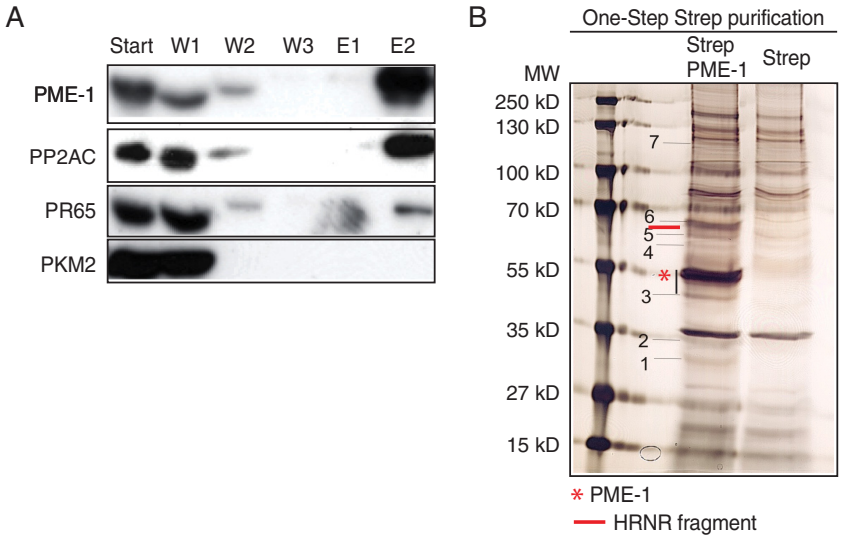

FIG. 4. **AP-MS Identification of PME-1 interactome.** (*A*) One-step strep-tag purification of PME-1 reveals an expected interaction with PP2A subunits PP2Ac and PR65. W: washes, E: elutions. (*B*) Silverstaining analysis of Streptactin affinity column purified proteins eluted from either StrepPME-1 or control strep tag expressing cells. Numbers refer to proteins bands subjected for MS analysis from both sample lanes.

abundance proteins could be present also in the corresponding bands from the Strep control lane, those also were analyzed by MS, and any protein that was identified from the Strep control lane were omitted from further analysis. Based on these criteria, the final library of putative PME-1 interacting proteins contained 49 proteins (Supplemental Table 7). Importantly, proteins in the PME-1 interactome library were not filtered based on the number of identified peptides and only a Mascot significance threshold of $p < .05$ was used to assess the reliability of AP-MS identification of interacting proteins. This was done purposely to challenge the capacity of RRP to dissociate between relevant and nonrelevant interactions even from low fidelity MS identification.

Evidence of RRPs Functionality in Relevance Ranking of AP-MS Interactome—Next, the newly identified PME-1 interactome, excluding the previously identified PME-1 interacting PP2A components (Supplemental Table 7), was subjected to RRP analysis. In addition, MAPK3 (ERK1) and AKT1 were included in the RRP library as internal controls representing known PME-1 effector proteins (11, 23). The relevance of the PC-3 cell model for assessing PME-1 interactome function was validated by robust inhibition of colony growth by PME-1 depletion (Supplemental Fig. 4). The results of individual RRP filtering steps for the PME-1 interactome and the list of final RRP ranks are shown in Supplemental Tables 8 and 9. RRP's improved power to dissociate between functionally relevant and nonrelevant proteins was validated also in this setting as the known PME-1 effectors AKT1 and MAPK3 showed up among the proteins with the most similar function to PME-1 (Fig. 5*A*).

Notably, except for AKT1 and MAPK3, the other proteins listed in Fig. *5A* have not been previously identified as PME-1 effectors. To assess the confidence of interaction between PME-1 and its top ranked RRP candidates, we analyzed the data with CRAPome (4), the contaminant repository from over 400 AP-MS experiments along with a computational tool allowing estimation of likelihood that an observed interaction is unspecific. As shown in Fig. 5*A*, most of the highest RRP ranking PME-1 interactors, except for chaperone protein HSPA8, were not frequently identified as contaminating proteins in previous AP-MS experiments using the Strep-Tactin affinity column that was used here for the isolation of PME-1 complex. Specificity of the interaction between PME-1 and its top ranked RRP candidates, except for LRRC8E, is also supported by analysis of MS data by SAINT analysis (3)(Fig. 5*A*). Importantly, we further validated interactions between PME-1 and two proteins, FDPS, and HRNR, by antibody-based detection from an independent Strep-PME-1 purification sample, whereas no enrichment of an unrelated protein ERp72 was found in Strep-PME-1 elution samples (Fig. 5*B*). HRNR interaction was identified from a protein band corresponding to about 60 kDa protein size, representing a known fragment of HRNR that is processed from full length 250 kDa protein (24) (Figs. 4*B* and 5*B*, red line). For FDPS, we show that whereas wild-type PME-1 does interact with FDPS, this interaction is greatly impaired with PME-1 R369D mutant that is defective in binding to PP2A catalytic subunit PP2Ac (Figs. 5*C* and 5*D*) (25). This further strengthens the evidence that RRP analysis can identify functionally relevant interacting proteins. We also validated protein interaction between PME-1 and Lamin A/C, as among the interacting proteins it showed the highest number of identified peptides and Mascot score (Fig. 5*E*). Based on insoluble nature of Lamin A/C, we used *in situ* proximity ligation assay for validation (Fig. 5*E*).

Although we have not proceeded to study the potential mechanisms by which this HRNR fragment contributes to PME-1 biology, its previously uncharacterized function in promoting cancer cell viability and its similarity with PME-1

A

RRP rank order	NCBI gene symbol	Peptides	Mascot	Rank summary	FunCoup	Validation	CRAPome Ave SC	SAINT
1	P4HB	4	82	-2,703209	0,174	-	not found	1
2	FDPS	2	38	-1,845824	NA	This study	not found	0,98
3	AKT1	NA	NA	-1,806180	NA	Ref. 23	NA	NA
4	MDH2	2	62	-1,676126	0,915	-	not found	0,98
5	HSPA8	6	70	-1,646056	0,181	n.d.	18,44	1
6	LRRC8E	1	36	-1,626584	NA	n.d.	not found	0
7	EEF2	6	38	-1,552933	0,607	Refs. 29, 30	1	1
8	MAPK3	NA	NA	-1,508755	0,833	Ref. 11	NA	NA
9	HRNR	3	83	-1,507430	NA	This study	4,31	0,98
10	LMNA	14	348	-1,133886	NA	This study	not found	1

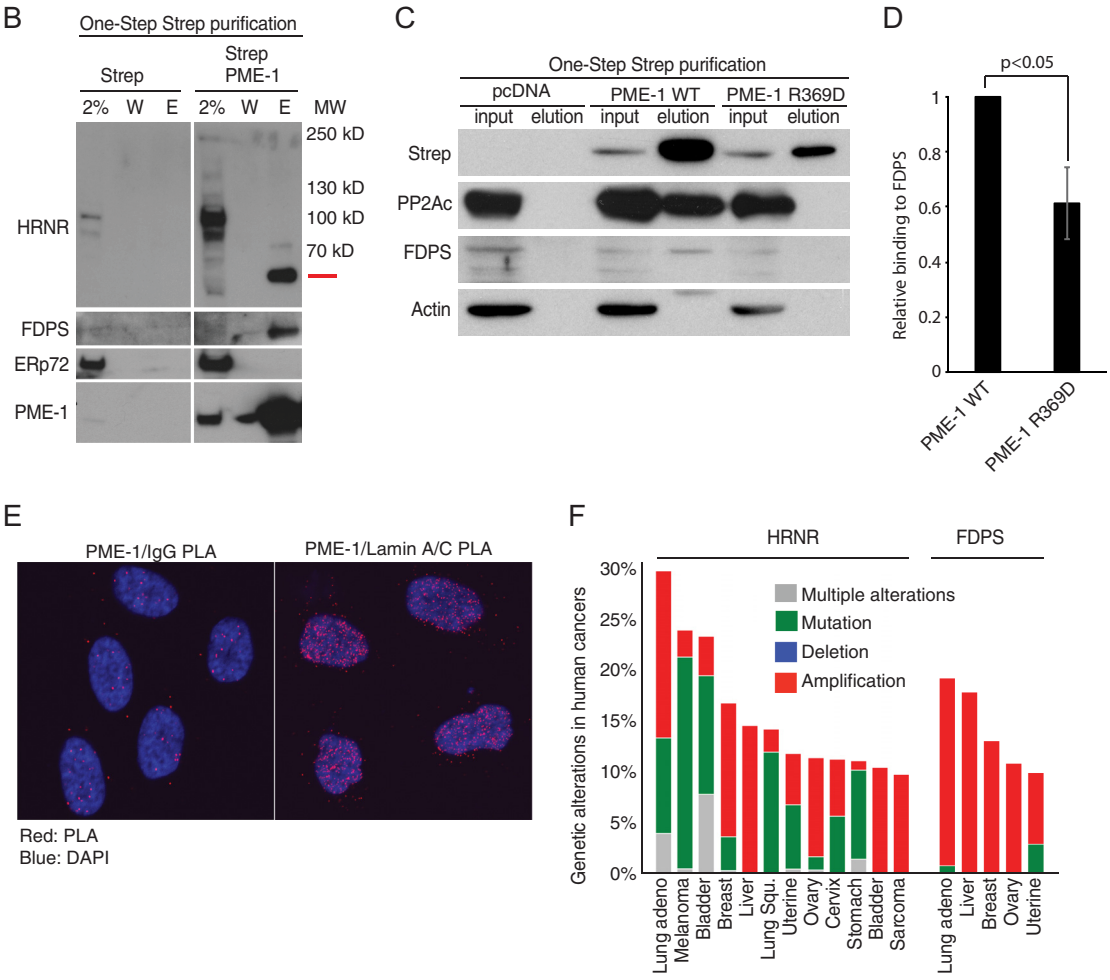

FIG. 5. **RRP analysis of PME-1 interactome.** (*A*) RRP ranking of top ten proteins with most similar function to PME-1. AKT1 and MAPK3 were included to RRP analysis as previously validated PME-1 effector genes (11, 23). FunCoup similarity index (min. 0, max. 1). NA, not applicable due to lack of sufficient database information. Validation indicates either physical or functional validation for indicated interaction. N.d., not determined, –, not observed. CRAPome analysis indicates for likelihood that the identified interaction is contamination. Ave SC: Average spectral counts (*B*) Validation of PME-1 interaction with either HRNR (60 kDa fragment) or FDPS. (*C*) Interaction between PME-1 and FDPS is dependent on PP2Ac binding of PME-1. PC-3 cells transfected with wild type of PP2Ac binding mutant of strep-PME-1 were subjected to Strep purification and WB. (D) Quantification of impact of PP2A binding to PME-1-FDPS interaction from panel *C*. Shown is mean ± S.D. of three independent experiment. T-test. (*E*) Proximity ligation assay (PLA) for interaction between PME-1 and Lamin A/C. (*F*) Genomic status of HRNR and FDPS across human cancer types based on cBio database (26).

oncoprotein function prompted us to validate its potential cancer relevance by using cBioPortal (26). Surprisingly, although previously thought to be a structural component of cornified epithelia (27), HRNR showed a very high degree of genomic changes in multiple human cancer types (Fig. 5*F*), further indicating its potential involvement in cancer biology.

Also, FDPS did show a high degree of amplifications in several human cancer types (Fig. 5*F*).

Expectedly, since FunCoup relies on integrating the existing data on protein interactions and several other types of evidence, something that is very scarce for PME-1, FunCoup analysis of the entire PME-1 interactome identified by Strep-tag purification was uninformative (Supplemental Table 10 and Fig. 5*A*). However, two genes among the top ten RRP candidates, MAPK3 (the positive control) and EEF2 (PP2A target protein) did show a high FunCoup index (Fig. 5*A* and Supplemental Table 10).

DISCUSSION

Large-scale protein interaction screens have revolutionized our understanding of the basic principles of how proteins are organized in large protein complex machineries (1, 28, 29). However, in many cases, translation of this information to novel functional paradigms has been challenging. This work presents an approach to tackle this burden by ranking the identified interactions, based on potential functional similarity of the putative interactors with the known function of the bait protein, rather than solely relying on qualitative and quantitative analysis of the interaction data.

RRP performance was validated by using data from two different types of protein interaction experiments, database interactome for Pin1 and newly identified AP-MS interactome for PME-1. RRP analysis of both of the interactomes resulted in enrichment of the already validated effector protein as top ranking RRP hits for both bait proteins. Regarding Pin1, we also demonstrated novel function for two of the identified proteins in regulating of c-Jun phosphorylation. Prior to this work, no interactome analysis has been published for PME-1. Among identified interacting proteins were components of PP2A complexes (Fig. 4*A*), indicating that the PME-1 interactome proteins analyzed by RRP are relevant for PME-1 biology. This conclusion is further supported by our demonstration that PME-1 binding to PP2Ac is relevant for PME-1′s association with FDPS (Figs. 5*C* and 5*D*). FDPS is a very interesting PME-1 effector candidate for follow-up as it regulates the ERK MAPK pathway activity downstream of RAS (30), and PME-1 was shown to promote ERK pathway activity upstream of MEK (11). On the other hand, although the S100 family protein HRNR cannot directly be connected to PME-1-regulated signaling based on very scarce functional information on HRNR, many S100 proteins do regulate kinase signaling and in particular S100A12 was very recently shown, similar to PME-1, to promote ERK pathway activity (31). On the other hand, association of PME-1 with Lamin A/C could be functionally related to the previously demonstrated essential role of A-type lamins for PP2A-mediated dephosphorylation of Rb (32). In addition, recent studies have shown that one of the top ranked PME-1 interacting proteins, EEF2, is a bona fide PP2A target protein (33, 34). These potential functional implications of identified PME-1 interactions, together with presented validation experiments, give future directions to better understand how PME-1 may function as an oncoprotein in human glioma and other malignancies (11, 35). In addition, the work reports function of over 100 genes in both malignant and nonmalignant prostate epithelial cells, providing a rich foundation for further analysis of cancer specificity of their function.

While many useful approaches such as CRAPome and SAINT have been developed to increase the confidence of dissection between copurifying proteins that are true interactors from those that are considered as contaminants, the philosophy of RRP is somewhat different. RRP does not assess the reliability of the observed protein interaction *per se*, but aims to help the researcher to rank the candidate proteins according to likelihood of an interaction being functionally relevant to the function of the bait. Therefore, the added benefit of using RRP is that once the functional relevance of the interacting protein has been demonstrated by RRP; this motivates a researcher to invest on thorough analysis of even troublesome protein interactions. As demonstrated here, not all the candidate protein interactions for PME-1 could be confirmed, which is typical for an AP-MS experiment, and we therefore encourage the use of a combination of RRP and SAINT or CRAPome for further filtering of the data and for selecting the candidate interactors that fulfill the both requirements, functional relevance and high confidence interaction detection. We also reason that RRP might be especially beneficial for identification of mechanisms that are regulated by more stochastic and weak interactions. As shown by our previous studies, they may lead to the discovery of an entirely new biological concept (1, 5, 6). This obviously requires that the identified interaction and its functional relevance are properly verified by subsequent experimentation or, as it is proposed here, filtered by RRP for their functional relevance. In the case of CIP2A, original identification was made from a single AP-MS purification yielding seven peptides with low Mascot score, and this has translated to over 100 publications establishing the protein as one of the most common cancer driver alterations across human cancers (5, 36, 37).

Importantly, analysis of Pin1 interactome with either RRP or FunCoup ranked the same top ten proteins as most relevant to Pin1 function. However, for analysis of interactomes of proteins such as PME-1 for which there is not sufficient database information available to enable the use of FunCoup or other existing filtering tools, RRP can be the tool of choice. Unlike FunCoup, RRP can also incorporate the cellular context information, such as a particular cell line or cancer type, and thereby enables context-specific functional similarity predictions. The RRP framework presented in this work consists of different functional and bioinformatics modules that have to be chosen depending on the nature of the biological question under study. Importantly, the relevance of modular nature of RRP is emphasized by the result that the majority of the top ten RRP ranked proteins from both interactomes would have

had much lower ranks if only the RNAi screen from the PC3 cell line would have been used as a functional filter (Supplemental Table 11). Therefore, RRP clearly offers an added value beyond the already existing bioinformatics (3, 4, 8) and RNAi approaches (38, 39). Based on the vast amount of gene expression data covering also all functionally nonannotated genes, RRP could in principle be used for any gene whose function can be addressed by an siRNA-based screening assay, including not only cell survival analysis but also a variety of high-content imaging based phenotypic screens. Regarding low costs of RNAi libraries compatible with a 384-well format, functional relevance screening as presented here may in fact be more cost efficient than purchase of various antibodies for interaction validation with proteins that might not functionally be relevant for the scientific question addressed. Naturally, there will be some phenotypes that are not RNAi compatible, but similar restrictions apply for all filtering tools.

In summary, the data presented here introduce an approach to address one of the major challenges in functional translation of high-content protein interaction data. The presented RRP platform is a versatile and cost-efficient modular filtering tool to help the researcher choose those interactors that most likely will contribute to the function of the bait protein of interest, either from the existing protein interaction databases or from AP-MS data.

Acknowledgments—We want to thank Taina Kalevo-Mattila for her excellent help in validation experiments and Dr. Maciej Lalowski for advice regarding SAINT analysis.

* This study was supported by funding from FIMM National Network for Molecular Medicine program, Academy of Finland (grants 252572 to JW, 272437, 269862, 279163 to TA, and 277293 to KW); Foundation for Finnish Cancer Institute (JW), Cancer Society of Finland (JW, TA and KW), and Jane and Aatos Erkko Foundation (KW). The authors declare no conflict of interest.

Ⓢ This article contains supplemental material Supplemental Tables 1–11 and Supplemental Figs. 1–4.

‡‡ These authors contributed equally to the paper.

§§ To whom correspondence should be addressed: Email: jukwes@utu.fi.

REFERENCES

1. Westermarck, J., Ivaska, J., and Corthals, G. L. (2013) Identification of protein interactions involved in cellular signaling. *Mol. Cell. Proteomics* **12,** 1752–1763
2. Wu, J., Vallenius, T., Ovaska, K., Westermarck, J., Mäkelä, T. P., and Hautaniemi, S. (2009) Integrated network analysis platform for protein–protein interactions. *Nature Methods* **6,** 75–77
3. Choi, H., Larsen, B., Lin, Z. Y., Breitkreutz, A., Mellacheruvu, D., Fermin, D., Qin, Z. S., Tyers, M., Gingras, A. C., and Nesvizhskii, A. I. (2011) SAINT: Probabilistic scoring of affinity purification-mass spectrometry data. *Nature Methods* **8,** 70–73
4. Mellacheruvu, D., Wright, Z., Couzens, A. L., Lambert, J. P., St-Denis, N. A., Li, T., Miteva, Y. V., Hauri, S., Sardiu, M. E., Low, T. Y., Halim, V. A., Bagshaw, R. D., Hubner, N. C., Al-Hakim, A., Bouchard, A., Faubert, D., Fermin, D., Dunham, W. H., Goudreault, M., Lin, Z. Y., Badillo, B. G., Pawson, T., Durocher, D., Coulombe, B., Aebersold, R., Superti-Furga, G., Colinge, J., Heck, A. J., Choi, H., Gstaiger, M., Mohammed, S., Cristea, I. M., Bennett, K. L., Washburn, M. P., Raught, B., Ewing, R. M., Gingras, A. C., and Nesvizhskii, A. I. (2013) The CRAPome: A contaminant repository for affinity purification-mass spectrometry data. *Nature Methods* **10,** 730–736
5. Junttila, M. R., Puustinen, P., Niemelä, M., Ahola, R., Arnold, H., Böttzauw, T., Ala-aho, R., Nielsen, C., Ivaska, J., Taya, Y., Lu, S. L., Lin, S., Chan, E. K., Wang, X. J., Grènman, R., Kast, J., Kallunki, T., Sears, R., Kähäri, V. M., and Westermarck, J. (2007) CIP2A inhibits PP2A in human malignancies. *Cell* **130,** 51–62
6. Mialon, A., Sankinen, M., Söderström, H., Junttila, T. T., Holmström, T., Koivusalo, R., Papageorgiou, A. C., Johnson, R. S., Hietanen, S., Elenius, K., and Westermarck, J. (2005) DNA topoisomerase I is a cofactor for c-Jun in the regulation of epidermal growth factor receptor expression and cancer cell proliferation. *Mol. Cell. Biol.* **25,** 5040–5051
7. Westermarck, J., Weiss, C., Saffrich, R., Kast, J., Musti, A. M., Wessely, M., Ansorge, W., Séraphin, B., Wilm, M., Valdez, B. C., and Bohmann, D. (2002) The DEXD/H-box RNA helicase RHII/Gu is a co-factor for c-Jun-activated transcription. *EMBO J.* **21,** 451–460
8. Schmitt, T., Ogris, C., and Sonnhammer, E. L. (2014) FunCoup 3.0: Database of genome-wide functional coupling networks. *Nucleic Acids Res.* **42,** D380–388
9. Ayala, G., Wang, D., Wulf, G., Frolov, A., Li, R., Sowadski, J., Wheeler, T. M., Lu, K. P., and Bao, L. (2003) The prolyl isomerase Pin1 is a novel prognostic marker in human prostate cancer. *Cancer Res.* **63,** 6244–6251
10. Ryo, A., Uemura, H., Ishiguro, H., Saitoh, T., Yamaguchi, A., Perrem, K., Kubota, Y., Lu, K. P., and Aoki, I. (2005) Stable suppression of tumorigenicity by Pin1-targeted RNA interference in prostate cancer. *Clin Cancer Res.* **11,** 7523–7531
11. Puustinen, P., Junttila, M. R., Vanhatupa, S., Sablina, A. A., Hector, M. E., Teittinen, K., Raheem, O., Ketola, K., Lin, S., Kast, J., Haapasalo, H., Hahn, W. C., and Westermarck, J. (2009) PME-1 protects extracellular signal-regulated kinase pathway activity from protein phosphatase 2A-mediated inactivation in human malignant glioma. *Cancer Res.* **69,** 2870–2877
12. Kilpinen, S., Autio, R., Ojala, K., Iljin, K., Bucher, E., Sara, H., Pisto, T., Saarela, M., Skotheim, R. I., Björkman, M., Mpindi, J. P., Haapa-Paananen, S., Vainio, P., Edgren, H., Wolf, M., Astola, J., Nees, M., Hautaniemi, S., and Kallioniemi, O. (2008) Systematic bioinformatic analysis of expression levels of 17,330 human genes across 9,783 samples from 175 types of healthy and pathological tissues. *Genome Biol.* **9,** R139
13. König, R., Chiang, C. Y., Tu, B. P., Yan, S. F., DeJesus, P. D., Romero, A., Bergauer, T., Orth, A., Krueger, U., Zhou, Y., and Chanda, S. K. (2007) A probability-based approach for the analysis of large-scale RNAi screens. *Nature Methods* **4,** 847–849
14. Johansen, L. D., Naumanen, T., Knudsen, A., Westerlund, N., Gromova, I., Junttila, M., Nielsen, C., Bottzauw, T., Tolkovsky, A., Westermarck, J., Coffey, E. T., Jäättelä, M., and Kallunki, T. (2008) IKAP localizes to membrane ruffles with filamin A and regulates actin cytoskeleton organization and cell migration. *J. Cell Sci.* **121,** 854–864
15. Junttila, M. R., Saarinen, S., Schmidt, T., Kast, J., and Westermarck, J. (2005) Single-step strep-tag purification for the isolation and identification of protein complexes from mammalian cells. *Proteomics* **5,** 1199–1203
16. Liu, G., Zhang, J., Larsen, B., Stark, C., Breitkreutz, A., Lin, Z. Y., Breitkreutz, B. J., Ding, Y., Colwill, K., Pasculescu, A., Pawson, T., Wrana, J. L., Nesvizhskii, A. I., Raught, B., Tyers, M., and Gingras, A. C. (2010) ProHits: Integrated software for mass spectrometry-based interaction proteomics. *Nature Biotechnol.* **28,** 1015–1017
17. Lee, H. K., Hsu, A. K., Sajdak, J., Qin, J., and Pavlidis, P. (2004) Coexpression analysis of human genes across many microarray data sets. *Genome Res.* **14,** 1085–1094
18. Shen, M., Stukenberg, P. T., Kirschner, M. W., and Lu, K. P. (1998) The essential mitotic peptidyl-prolyl isomerase Pin1 binds and regulates mitosis-specific phosphoproteins. *Genes Dev.* **12,** 706–720
19. Proteau, A., Blier, S., Albert, A. L., Lavoie, S. B., Traish, A. M., and Vincent, M. (2005) The multifunctional nuclear protein p54nrb is multiphosphorylated in mitosis and interacts with the mitotic regulator Pin1. *J. Mol. Biol.* **346,** 1163–1172
20. Lavoie, S. B., Albert, A. L., Handa, H., Vincent, M., and Bensaude, O. (2001) The peptidyl-prolyl isomerase Pin1 interacts with hSpt5 phosphorylated

by Cdk9. *J. Mol. Biol.* **312,** 675–685
21. Westermarck, J. (2010) Regulation of transcription factor function by targeted protein degradation: An overview focusing on p53, c-Myc, and c-Jun. *Meth. Mol. Biol.* **647,** 31–36
22. Wulf, G. M., Ryo, A., Wulf, G. G., Lee, S. W., Niu, T., Petkova, V., and Lu, K. P. (2001) Pin1 is overexpressed in breast cancer and cooperates with Ras signaling in increasing the transcriptional activity of c-Jun towards cyclin D1. *EMBO J.* **20,** 3459–3472
23. Jackson, J. B., and Pallas, D. C. (2012) Circumventing cellular control of PP2A by methylation promotes transformation in an Akt-dependent manner. *Neoplasia* **14,** 585–599
24. Fleming, J. M., Ginsburg, E., Oliver, S. D., Goldsmith, P., and Vonderhaar, B. K. (2012) Hornerin, an S100 family protein, is functional in breast cells and aberrantly expressed in breast cancer. *BMC Cancer* **12,** 266
25. Xing, Y., Li, Z., Chen, Y., Stock, J. B., Jeffrey, P. D., and Shi, Y. (2008) Structural mechanism of demethylation and inactivation of protein phosphatase 2A. *Cell* **133,** 154–163
26. Cerami, E., Gao, J., Dogrusoz, U., Gross, B. E., Sumer, S. O., Aksoy, B. A., Jacobsen, A., Byrne, C. J., Heuer, M. L., Larsson, E., Antipin, Y., Reva, B., Goldberg, A. P., Sander, C., and Schultz, N. (2012) The cBio cancer genomics portal: An open platform for exploring multidimensional cancer genomics data. *Cancer Discovery* **2,** 401–404
27. Henry, J., Hsu, C. Y., Haftek, M., Nachat, R., de Koning, H. D., Gardinal-Galera, I., Hitomi, K., Balica, S., Jean-Decoster, C., Schmitt, A. M., Paul, C., Serre, G., and Simon, M. (2011) Hornerin is a component of the epidermal cornified cell envelopes. *FASEB J.* **25,** 1567–1576
28. Glatter, T., Wepf, A., Aebersold, R., and Gstaiger, M. (2009) An integrated workflow for charting the human interaction proteome: Insights into the PP2A system. *Mol. Systems Biol.* **5,** 237
29. Stelzl, U., Worm, U., Lalowski, M., Haenig, C., Brembeck, F. H., Goehler, H., Stroedicke, M., Zenkner, M., Schoenherr, A., Koeppen, S., Timm, J., Mintzlaff, S., Abraham, C., Bock, N., Kietzmann, S., Goedde, A., Toksöz, E., Droege, A., Krobitsch, S., Korn, B., Birchmeier, W., Lehrach, H., and Wanker, E. E. (2005) A human protein–protein interaction network: A resource for annotating the proteome. *Cell* **122,** 957–968
30. Reilly, J. F., Martinez, S. D., Mickey, G., and Maher, P. A. (2002) A novel role for farnesyl pyrophosphate synthase in fibroblast growth factor-mediated signal transduction. *Biochem. J.* **366,** 501–510
31. Kang, J. H., Hwang, S. M., and Chung, I. Y. (2015) S100A8, S100A9 and S100A12 activate airway epithelial cells to produce MUC5AC via extracellular signal-regulated kinase and nuclear factor-kappaB pathways. *Immunology* **144,** 79–90
32. Van Berlo, J. H., Voncken, J. W., Kubben, N., Broers, J. L., Duisters, R., van Leeuwen, R. E., Crijns, H. J., Ramaekers, F. C., Hutchison, C. J., and Pinto, Y. M. (2005) A-type lamins are essential for TGF-beta1 induced PP2A to dephosphorylate transcription factors. *Human Mol. Genetics* **14,** 2839–2849
33. Yang, C. W., Lee, Y. Z., Hsu, H. Y., Wu, C. M., Chang, H. Y., Chao, Y. S., and Lee, S. J. (2013) c-Jun-mediated anticancer mechanisms of tylophorine. *Carcinogenesis* **34,** 1304–1314
34. McDermott, M. S., Browne, B. C., Conlon, N. T., O'Brien, N. A., Slamon, D. J., Henry, M., Meleady, P., Clynes, M., Dowling, P., Crown, J., and O'Donovan, N. (2014) PP2A inhibition overcomes acquired resistance to HER2 targeted therapy. *Mol. Cancer* **13,** 157
35. Wandzioch, E., Pusey, M., Werda, A., Bail, S., Bhaskar, A., Nestor, M., Yang, J. J., and Rice, L. M. (2014) PME-1 modulates protein phosphatase 2A activity to promote the malignant phenotype of endometrial cancer cells. *Cancer Res.* **74,** 4295–4305
36. Khanna, A., and Pimanda, J. E. (2015) Clinical significance of cancerous inhibitor of protein phosphatase 2A (CIP2A) in human cancers. *Int. J. Cancer* Jan 13. [Epub ahead of print]
37. Khanna, A., Pimanda, J. E., and Westermarck, J. (2013) Cancerous inhibitor of protein phosphatase 2A, an emerging human oncoprotein and a potential cancer therapy target. *Cancer Res.* **73,** 6548–6553
38. Ramage, H. R., Kumar, G. R., Verschueren, E., Johnson, J. R., Von Dollen, J., Johnson, T., Newton, B., Shah, P., Horner, J., Krogan, N. J., and Ott, M. (2015) A combined proteomics/genomics approach links hepatitis C virus infection with nonsense-mediated mRNA decay. *Mol. Cell* **57,** 329–340
39. Friedman, A. A., Tucker, G., Singh, R., Yan, D., Vinayagam, A., Hu, Y., Binari, R., Hong, P., Sun, X., Porto, M., Pacifico, S., Murali, T., Finley, R. L., Jr., Asara, J. M., Berger, B., and Perrimon, N. (2011) Proteomic and functional genomic landscape of receptor tyrosine kinase and RAS to extracellular signal-regulated kinase signaling. *Sci. Signal.* **4,** rs10